RSC Advances

This is an *Accepted Manuscript*, which has been through the Royal Society of Chemistry peer review process and has been accepted for publication.

Accepted Manuscripts are published online shortly after acceptance, before technical editing, formatting and proof reading. Using this free service, authors can make their results available to the community, in citable form, before we publish the edited article. This *Accepted Manuscript* will be replaced by the edited, formatted and paginated article as soon as this is available.

You can find more information about *Accepted Manuscripts* in the Information for Authors.

Please note that technical editing may introduce minor changes to the text and/or graphics, which may alter content. The journal's standard Terms & Conditions and the Ethical guidelines still apply. In no event shall the Royal Society of Chemistry be held responsible for any errors or omissions in this *Accepted Manuscript* or any consequences arising from the use of any information it contains.

ROYAL SOCIETY OF CHEMISTRY

www.rsc.org/advances

Amphoteric nanoporous polybenzimidazole membrane with extremely low crossover for a vanadium redox flow battery

Sandip Maurya, Sung-Hee Shin, Ju-Young Lee, Yekyung Kim, Seung-Hyeon Moon*

School of environmental science and engineering, Gwangju Institute of Science and Technology (GIST), 261 Cheomdan-Gwagiro, Gwangju 61005, Republic of Korea

* Corresponding author: Professor Seung-Hyeon Moon, E-Mail: shmoon@gist.ac.kr, Phone: +82-62-715-2435, Fax: +82-62-715-2434

RSC Advances Accepted Manuscript

Abstract:

We report amphoteric polybenzimidazole (PBI) membranes with tailored nanoporous structures for vanadium redox flow batteries (VRFBs). The amphoteric nanoporous membrane has restricted the crossover of vanadium species and instantaneously allowed for the transport of protons owing to the positively charged polybenzimidazolium polymer backbone. The selected membrane shows a proton/vanadium (H/V) selectivity of about 133, which is considerably higher than those stated in previous reports. This reflects its high coulombic efficiency of 99.4%, energy efficiency of 78.2%, and low capacity decay rate of 0.27% per cycle when compared to 93.0%, 78.9%, and 0.58% per cycle of Nafion-117, respectively.

Keywords: Nanoporous membrane; amphoteric membrane; vanadium redox flow battery; polybenzimidazole membrane; anion exchange membrane.

RSC Advances Accepted Manuscript

1. Introduction

Among the available current electrochemical energy storage technologies, vanadium redox flow batteries (VRFBs) are the leading candidate for large-scale sporadic energy storage due to their long life cycle, low cost per kilowatt, and independent energy and power outputs [1]. The VRFB was pioneered at the University of New South Wales, Australia by Maria Skyllas-Kazacos in 1985 [2,3]. The VRFB is unique because both positive ($V_{(IV)}/V_{(V)}$ redox couple) and negative ($V_{(II)}/V_{(III)}$) electrolytes are derived from the $VOSO_4$ (vanadyl sulfate) and dissolved in H_2SO_4 (sulfuric acid), though different in oxidation states. During charge and discharge processes, electroneutrality is maintained by the transport of protons and anions through the separator [4].

In the VRFB cell, an ion exchange membrane offers electron insulation and ion transport from anode to cathode or vice versa. Moreover, the ion exchange membrane separates both compartments to avoid the mixing of anolyte and catholyte solutions. Ideally, membranes for VRFBs should possess good ionic conductivity and a low crossover of active species (i.e., ion selectivity) with high chemical and mechanical stabilities in a highly acidic environment [5–7]. Perfluorosulfonic acid (i.e., Nafion®)-based cation exchange membranes are currently widely used in VRFBs thanks to their excellent chemical stability and good proton conductivity [8]. Nonetheless, critical issues associated with an intense crossover of vanadium ions and the cost of membranes have yet to be solved [6]. Recently, most research has been concentrated on the cheaper non-fluorinated hydrocarbon-based sulfonated cation exchange membranes and quaternized anion exchange membranes (AEMs) [9–11]. AEMs have drawn considerable attention, as they exhibit a lower vanadium crossover than sulfonated cation exchange membranes due to the Donnan exclusion phenomena (electrostatic repulsion between positive

RSC Advances Accepted Manuscript

functional groups and vanadium ions) [12]. Sulfonation or quaternization of the inert polymer often results in a low chemical stability in an oxidative vanadium solution [6]. The reagents and leftovers of these chemical reactions are hazardous to the environment. Thus, the development of alternative membranes becomes the top priority for the commercialization of VRFB technology.

Hypothetically, any porous film that selectively allows transport of supporting electrolytes can be used as separators in VRFBs [13]. Few studies have been carried out on cheap microporous Daramic® separators for VRFBs where the reasonable performances of 95% coulombic efficiency (CE) and 83% energy efficiency (EE) were achieved [14,15]. Recently, Zhang et al [16,17] and Wei et al [18] presented the viability of nanoporous membranes with sensible VRFB performance. All these porous membranes have shown better selectivity toward protons than vanadium ions because protons move faster compared to bulky vanadium ions in an aqueous electrolyte solution. Porous membranes have shown low capacity decay when compared to Nafion membranes, though their low CE (~93%) makes them a less preferred choice. In another attempt, Zhang et el [19] reported the spongy AEM, however, these membranes also encounter low CE (~94% at 40 mA cm^{-2} current density). Major setback for Spongy AEMs are the need of chloromethylation and quaternization reactions for anion exchange functionality that requires the use of hazardous chloromethyl methyl ether and terimethyl amine. However, no information about capacity decay is given; they suffer from the slow but definite crossover of vanadium ions. Recently, Zhou et al [20] reported polybenzimidazole based membranes with improved performance in VRFBs, however, the description about the improved performance is remain obscured.

Herein, we combine the benefits of AEMs and nanoporous membranes using polybenzimidazole (PBI) polymer that exhibit low crossover, high EEs, and the effective

RSC Advances Accepted Manuscript

transport of charge carriers. This novel approach eliminates the need of chloromethylation and quaternization reaction for anion exchange functionality. Subsequently, we report a method to develop amphoteric nanoporous PBI membranes by the simple solution casting. The reasons behind the high performance of PBI membranes are explicated by means of the membrane potential. The VRFB based on new PBI membrane showed a CE of 99.4%, EE of 78.2%, and low capacity decay rate of 0.27% per cycle at 40 $mAcm^{-2}$. To the best knowledge of the authors, this is the first time to exploit the amphoteric properties of nanoporous PBI membranes in VRFBs.

2. Experimental

2.1 Materials

Polyphosphoric acid (115%), terephthalic acid, polyethylene glycol (PEG, MW: 400 Da), and dimethylacetamide (DMAc) were purchased from Sigma Aldrich Inc., USA. 3,3'-diaminobenzidine and azelaic acid were purchased from Alfa Aesar, UK. Calcium chloride and ammonia solution (28%) were procured from OCI Chemicals Ltd., Korea. The reagents were analytical grade and used as received without further purification.

2.2. Synthesis of the polybenzimidazole polymer

The PBI polymer was synthesized by polycondensation polymerization using polyphosphoric acid, which acts as a solvent and dehydrating agent as well. Typically, a three-necked round-bottom flask equipped with an overhead mechanical stirrer, N_2 gas inlet, and $CaCl_2$ tube was filled with 3,3'-diaminobenzidine (2.5 g, 0.01167 mole) and 100 g of polyphosphoric acid, and the temperature was raised to 140 ^oC for 1–2 h. Further, an equimolar

RSC Advances Accepted Manuscript

quantity of dicarboxylic acid (1:1 ratio of terephthalic acid and Azelaic acid, 0.01167 mole) was added. The temperature of the reactant solution was gradually increased to 195 ^{o}C and maintained for 20 h. The obtained viscous polymer solution was then poured into cold water. The precipitated polymer was washed several times with water until a neutral pH was achieved. Then, the polymer was kept in a 10% ammonia solution overnight with constant stirring. After the alkaline treatment, the polymer was washed several times with water and dried in an oven at 110 ^{o}C for 24 h. Synthesis of PBI polymer was confirmed by the ^{1}H NMR and FT-IR analysis **(Supporting information, SI, Fig. 1S and 2S)**

2.3. Fabrication of nanoporous PBI membranes

The nanoporous PBI membranes were fabricated by the solution casting method. The PBI polymer was dissolved in DMAc to obtain an 8 wt% polymer solution at 100 ^{o}C. Then, a pre-determined amount of PEG was added to the polymer solution **(SI, Table 1S)** to prepare the casting solution. The polymer solutions were cast as thin films on clean glass plates using a membrane-casting unit, and dried at 110 ^{o}C for 12 h. The resultant membranes were washed thoroughly with water to remove the PEG from the membrane matrix and stored in deionized water.

2.4. Membrane characterizations

The morphology of nanoporous PBI membranes was investigated using scanning electron microscope (SEM, Hitachi S-4700). The membrane samples were dried at room temperature prior to analysis. Pore characteristics were examined by mercury intrusion porometry (Micromeritics Instruments Corp, WIN9400 series).

RSC Advances Accepted Manuscript

The ionic conductivity of the membranes was determined by measuring membrane electrical resistance (MER) in 0.5 M H_2SO_4 solution using two-probe clip-cell. The ionic conductivity was calculated by the equation below:

$$Ionic\ conductivity\ (S\ cm^{-1}) = \frac{L\ (cm)}{MER\ (\Omega cm^2)}$$

The transport number of nanoporous PBI membranes was determined by EMF method using a two-chamber diffusion cell equipped with a pair of Ag/AgCl reference electrodes. Transport numbers are calculated using the below equations [21]:

$$E_m = (2t_+ - 1)\frac{RT}{F} ln\frac{a_2}{a_1}$$

(when 1:1 valance electrolyte used such as KCl)

$$E_m = \left(\frac{3}{2}t_+ - 1\right)\frac{RT}{F} ln\frac{a_2}{a_1}$$

(when 2:1 valance electrolyte used such as H_2SO_4)

$$t_+ + t_- = 1$$

where a_1 and a_2 are the mean activities of the dilute and concentrated solutions, respectively; R is the universal gas constant; T is the temperature; F is the Faraday constant; and t_+ and t_- are the transport numbers of the cation and anion in the membrane, respectively.

The transport number was measured at various pH values using a 0.1 M and 0.5 M KCl solution where the pH was maintained using 0.5 M H_2SO_4 or 0.5 M NaOH solutions. The transport numbers of the protons were measured using 0.01 M and 0.05 M H_2SO_4.

2.5. A vanadium redox flow cell test

The VRFB single cell test was carried out using a 1.0 M $VOSO_4$– 2.5 M H_2SO_4 electrolyte solution in the lab-made flow cell. Two graphite plates and gold coated copper plates

RSC Advances Accepted Manuscript

act as current collector. Thermally treated graphite felt (500 ^{o}C for 5 hours in the air) was used as an electrode in both chambers. The membrane (6 cm^2) was sandwiched between electrodes and current collectors. Twenty ml of 1 M V^{3+} and V^{4+} in 2.5 M H_2SO_4 were used as negative and positive electrolyte, respectively. Flow rate of electrolytes was maintained at 8 ml/min throughout the experiment. The cycling test was performed at a current density of 40, 60, 80 and 100 mA cm^{-2} and cut-off voltages have been fixed at 0.8V and 1.6V for Nafion-117 and PBI-10% whereas 0.4V and 2.0V for PBI-0% due to its high area resistance using battery cycler (Scribner Associates, 580 Battery Test System).

3. Results and Discussions

3.1. Fabrication of nanoporous membranes

The nanoporous structure is formed by adding polyethylene glycol (PEG) into a casting solution; it leaves pores in the polymer matrix upon washing. Moreover, the interaction of protons with a benzimidazole ring in a PBI polymer forms a benzimidazolium cation, which further implants the properties of AEMs and that is also without undergoing chloromethylation and quaternization reactions. The pore size of the membranes was regulated by the varying amount of PEG from 0–10 wt%. The six membranes by adding 0, 2, 4, 6, 8, and 10% PEG were synthesized, and they were denoted as PBI-0% to PBI-10% according to the PEG content **(SI, Table 1S)**. The morphology of the membrane was analyzed by SEM micrographs. The PBI-0% to PBI-6% membranes showed a dense structure, while the PBI-8% and PBI-10% membranes showed a porous structure, owing to the relatively higher amount of PEG in a casting solution **(Fig. 1).** The average pore size and total pore area for the PBI-6%, PBI-8%, and PBI-10%

RSC Advances Accepted Manuscript

membranes were 98, 41, and 21 nm and 16.08, 110.26, and 140.18 $m^2 g^{-1}$, respectively **(SI, Table 2S).**

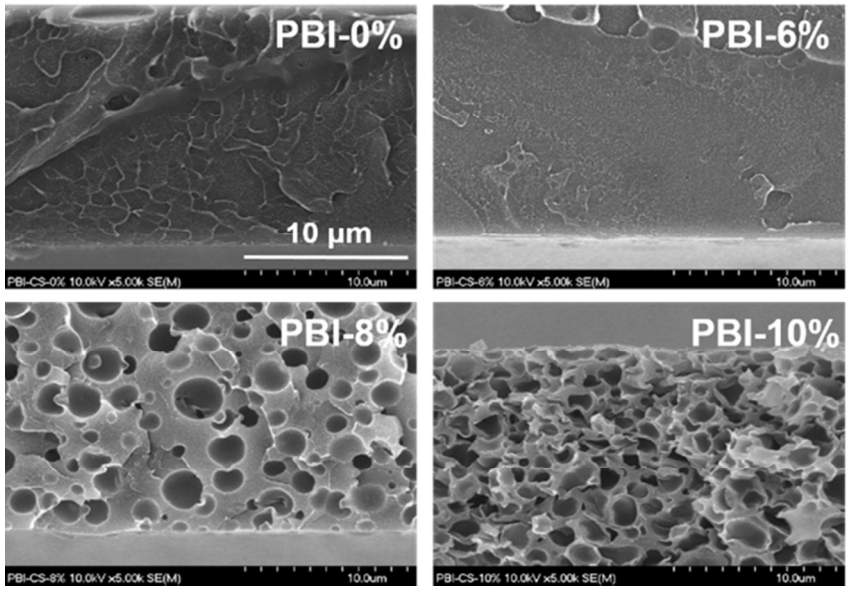

Figure 1. FE-SEM images of cross-section of membranes.

3.2. Characterizations of nanoporous membranes

The ionic conductivity values are consistent with the amount of PEG added for porosity. The PBI-10% membrane showed a conductivity of 1.61 mS cm^{-1}, which is considerably higher than 0.55 mS cm^{-1}, as shown by the non-porous PBI-0% membrane (**SI, Fig. 3S**). Also, the membrane electrical resistances for the PBI-0% and PBI-10% membrane are 4.72 and 1.92 Ω cm^2, respectively which is in good agreement with ionic conductivity values. In general, widely used Nafion-117 for VRFB application possess the MER between 0.2 - 0.3 Ω cm^2 depending on the measurement techniques [22].

The H/V selectivity was probed by measuring the relative diffusion of the proton and vanadium ions as described elsewhere [16,17]. A linear relationship between time and the concentration of protons and VO^{2+} ions is shown in Fig. 4S.

RSC Advances Accepted Manuscript

Table 2. H/V selectivity of the porous membranes.

Membrane	Thickness, µm	Diffusion rate, x 10^{-7} cm^2 min^{-1}		H/V selectivity
		H^+	VO^{2+}	
PBI-6%	28	43.9	0.23	190.8
PBI-8%	38	53.3	0.38	140.3
PBI-10%	45	156.0	1.17	133.3

Protons have exhibited a significantly higher diffusion rate than VO^{2+} **(Table 2)**. The PBI-10% membrane showed an H/V selectivity of ~133, which is lower than other porous membranes *i.e.* PBI-6% and PBI-8% membranes. This could be attributed to the higher diffusion rate of VO^{2+} due to the large pore area despite a narrow pore diameter. Interestingly, the H/V selectivity of the PBI membranes is significantly higher than the values reported in the literature, which range between 6.9 and 55.6 [16–18]. In general, a different mobility of protons and VO^{2+} in the aqueous electrolyte leads to the separation of the ions. The highly mobile and tiny protons diffuse faster than vanadium ions in RFB cells, which imparts the apparent selectivity of the protons to porous separators [4]. This feature was exploited by previous researchers to show a new prospect of nanoporous membranes in RFB applications; however, the larger pores assist in the diffusion of vanadium ions, which lowers the selectivity of the membranes.

The unusually high H/V selectivity of PBI nanoporous membranes was investigated by measuring the transport number by means of the membrane potential [21,23]. As shown in **Fig. 2**, the transport numbers of the PBI-10% membrane were measured in acidic, neutral, and alkaline pH values. When the PBI-10% membrane was in a neutral solution, the transport number for the anion was 0.94, which is comparable to commercial AEMs. The high anion transport number represents that anions preferentially transport through porous membranes. PBI membranes have retained transport behaviors in an acidic solution, as the transport number of the

RSC Advances Accepted Manuscript

anions was 0.84 at pH 2. The reduction in the transport number is due to the competitive transport of protons by diffusion. In other words, at neutral and acidic pH values, PBI porous membranes purely act as anion exchangers and therefore, it becomes more difficult for cations to pass through membranes. Interestingly, in the alkaline solution (pH 12), the anion transport number significantly decreased to 0.20. The low anion transport number values represent that the porous PBI-10% membrane favorably allows for the transport of cations at an alkaline pH. The amphoteric behavior of the PBI-10% membrane could be explained by the ionic interaction of the benzimidazole ring with proton and hydroxide ions **(Fig. 3)**. The benzimidazole unit of the PBI polymer contains two types of nitrogen: =N- and –NH-, where the partial charges were negative and positive, respectively [24,25]. The overall charge distribution neutralizes due to inter-ionic interactions with the neighbor benzimidazole ring. These interactions are strong in the PBI polymer with a rigid aromatic backbone, such as m-PBI [26]. Therefore, m-PBI-based membrane shows almost no selectivity toward ions in a neutral solution **(SI, Fig. 5S (a))**. However, the PBI-10% membrane consists of a relatively flexible aliphatic-aromatic polymer backbone; therefore, the benzimidazole ring is available for an ionic interaction with electrolyte solutions. The highly mobile protons preferably interact with the benzimidazole ring and therefore, the PBI-10% membrane act as an anion exchanger, even at a neutral pH. The ionic interaction of protons becomes significant at an acidic pH; as a result, the PBI-10% membrane becomes positively charged due to benzimidazolium cations. This positively charged membrane mutually repels cations from the electrolyte solution. This was altered in an alkaline solution, where a high concentration of hydroxide ions transforms it to cation selective, owing to negatively charged benzimidazole anions. A similar behavior was also observed for m-PBI membranes **(SI, Fig.5S))**.

RSC Advances Accepted Manuscript

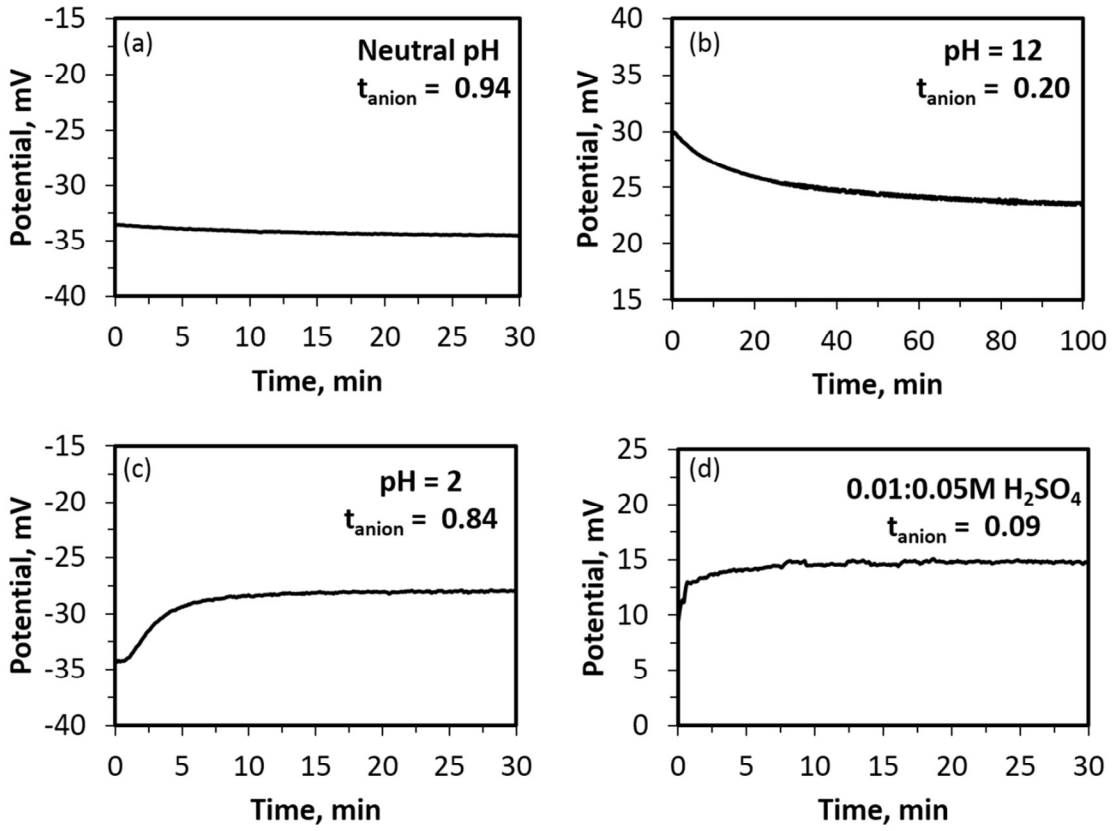

Figure 2. Comparison of anion transport behaviors in different types of electrolyte solutions: (a) 0.1 M and 0.5 M KCl solution at a neutral pH, (b) 0.1 M and 0.5 M KCl solution at pH 12, (c) 0.1 M and 0.5 M KCl solution at pH 2, and (d) 0.01 M and 0.05 M H_2SO_4 solution.

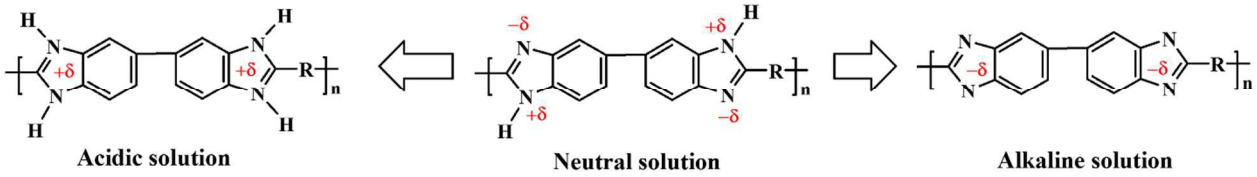

Figure 3. Effect of solution pH on the PBI membranes

In **Fig. 2(d)**, the anion transport number values for the PBI-10% membrane between 0.01 M and 0.05 M of the H_2SO_4 solution was 0.20. The increased cation selectivity of the PBI-10% membrane in an acidic solution is attributed to the relatively higher mobility of protons, which is 4.757 compared to sulfate at 0.544 [27,28]. The high diffusion of protons through the membranes

RSC Advances Accepted Manuscript

has been well known in dialysis, owing to its small atomic size and weight. To achieve electroneutrality in practical VRFB applications, not only sulfate ions, but also protons are simultaneously transported through the porous PBI-10% membrane, owing to the high proton transport number. Therefore, it was hypothesized that the PBI-10% membrane will act as an AEM to restrict the permeation of vanadium ions. Simultaneously, electroneutrality will be balanced by the transport of protons and sulfate ions from opposite compartments through the membrane.

The chemical stability of membranes was evaluated in the 1.0 M VO_2^+– 2.5 M H_2SO_4 electrolyte solution. The amount of VO^{2+} (where vanadium has +4 oxidation state) in the spent solution, formed by the reduction of VO_2^+, is determined by UV/Vis analysis **(SI, Fig. 6S).** As shown in **SI**, neither the VO^{2+} concentration nor the weight of the membranes in the solution change significantly with time. In addition, Nafion-117 showed marginally better chemical stability, on the other hand, PBI membrane showed the excellent chemical stability than the hydrocarbon based sulfonated polymers [29]. However, the slight loss in the apparent dimensional stability of PBI-10% indicates degradation of membrane by unknown degradation reaction pathway **(SI, Fig. 7S)**.

3.3. All vanadium redox flow battery single cell test

The actual performance of membranes is presented in **Fig. 4(a)**. The EE of PBI membranes, increased dramatically from 47.9% to 78.2% for PBI-0% to PBI-10% membranes. The PBI-10% membrane exhibited a CE of 99.4%, voltage efficiency (VE) of 78.6%, and EE of 78.2% at a current density of 40 mA cm^{-2}, as shown in **Fig. 4(a).** The single cell with the Nafion-117 membrane showed a 93.0% CE, 84.9% VE, and 78.9% EE under equivalent conditions. The

RSC Advances Accepted Manuscript

lower VE of PBI-0% and PBI-10% membrane is attributed to the low ionic conductivity, which increased the cell resistance in RFBs. The *in situ* cell resistance for PBI-0%, PBI-10% and Nafion-117% are 6.34, 3.31 and 0.54 Ω at 2.0 KHz, respectively which is in accordance with the voltage efficiency. The lower CE of Nafion-117 is due to the high crossover of vanadium ions through the negatively charged matrix. The PBI membranes have shown an exceptionally high impermeability toward positively charged vanadium ions, which is realized from 95.0% and 99.4% CE of the PBI-0% (thickness: 16 μm) and PBI-10% (thickness: 45 μm) membranes, respectively **(SI, Fig. 8S)**.

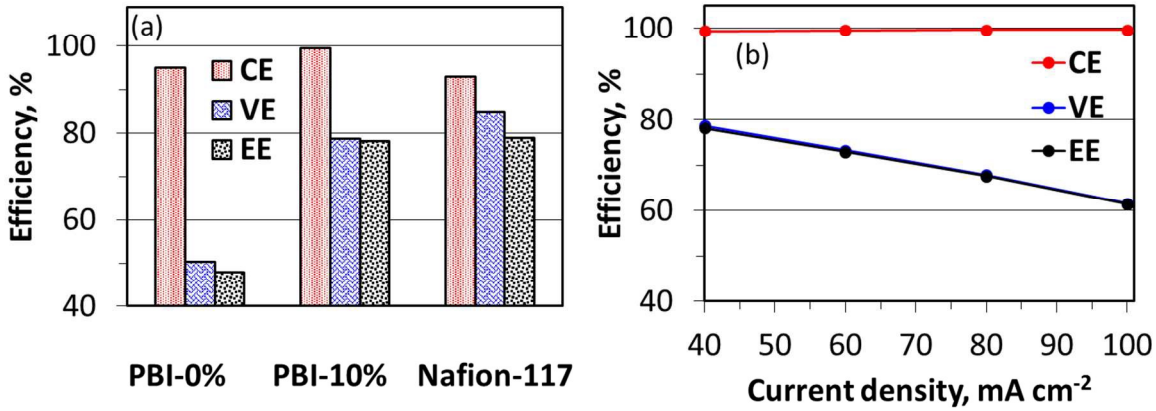

Figure 4. VRFB single cell performance of the PBI membrane in a 1.0 M $VOSO_4$– 2.5 M H_2SO_4 electrolyte solution: (a) charge–discharge cycling performance at 40 mA cm^{-2}; (b) PBI-10% performance at various current densities.

The CEs of PBI membranes are consistent regardless of their thinness and current density, which is attributed to the positively charged polybenzimidazolium backbone doused with sulfuric acid **(SI, Fig. 8S)**. The CE of the PBI-10% membrane is comparable with those of the AEMs, where a strong positive charge repels the vanadium ions [30]. A higher CE of a PBI

RSC Advances Accepted Manuscript

membrane confirms the versatility of PBI membranes that reject the vanadium ions at an acidic pH. The single cell performance of PBI-10% for various current densities is shown in **Fig. 4(b)**. The CE is slightly improved and reaches to 99.4% from 99.6% with the increase in current density from 40 $mAcm^{-2}$ to 100 $mAcm^{-2}$, respectively. This behavior is observed also for PBI-0% and Nafion-117 membranes and it could be attributed to the low vanadium crossover at higher current densities.

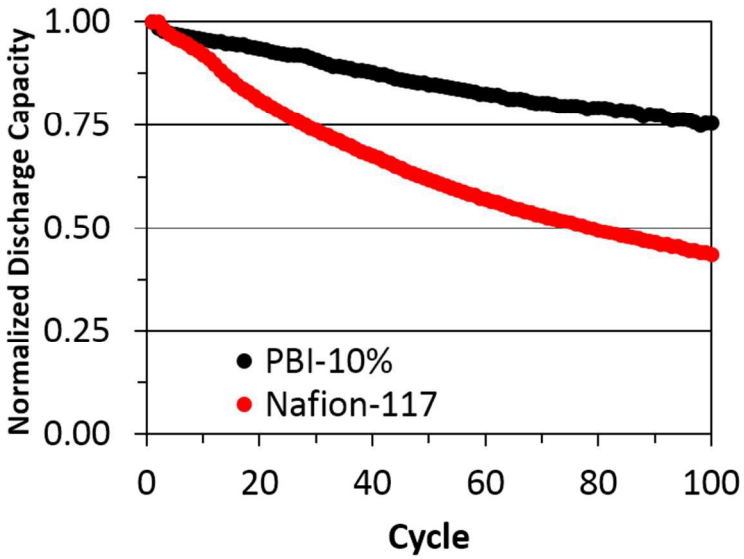

Figure 5. Capacity decay with cycle for PBI-10% and Nafion-117 membranes.

Nafion membranes suffer from the serious crossover of vanadium ions, which leads to an electrolyte imbalance because the long-term cycling stability of the VRFB system is collapsed [8]. Therefore, frequent electrolyte balancing is needed, which increases not only the complexity but also the cost of operations. The PBI-10% membrane exhibited excellent initial charge and discharge capacities of 15.74 and 15.09 Ah L^{-1}, respectively. On the other hand, the Nafion-117 membrane demonstrated initial charge and discharge capacities of 11.70 and 10.96 Ah L^{-1}, respectively at 40 mA cm^{-2}. The discharge capacity of the PBI-10% membrane was higher than that of the Nafion-117 membrane. Moreover, during cycling operations, the discharge capacity

RSC Advances Accepted Manuscript

of the Nafion-117 membrane decayed constantly at a rate of 0.58 % per cycle compared to 0.27% per cycle of the PBI-10% membrane (**Fig. 5**). The slow rate of capacity decay of the porous PBI-10% membrane is advantageous for long-term VRFB operations without the need of repeated electrolyte rebalancing.

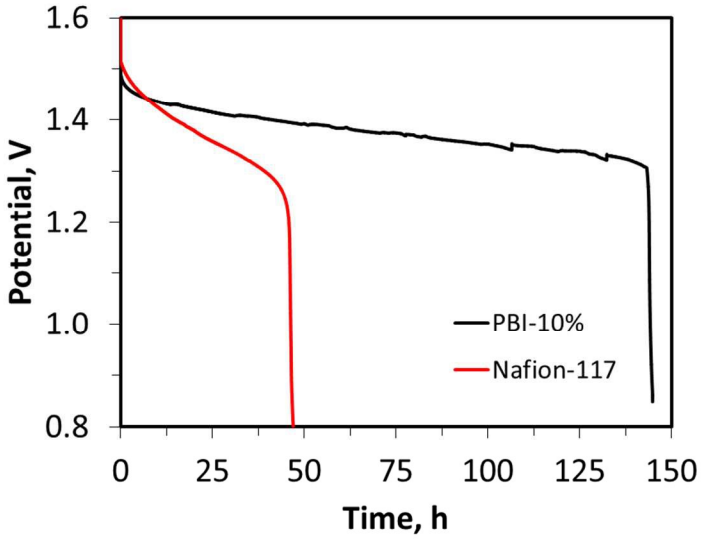

Figure 6. OCV decay curve for self-discharge experiments.

The OCV decay curves are displayed in **Fig. 6**, which reflect the depletion of charged vanadium species owing to the crossover in VRFBs. The self-discharge for Nafion-117 lasts 45 h, respectively, whereas the PBI-10% membrane showed a delayed self-discharge that lasts about 140 h. The extremely low permeability of vanadium ion confirms the porous PBI membranes could be the utmost solution to solving the long-queued problems associated with VRFBs. In addition, these results are in accordance with H/V selectivity and the hypothesis postulated.

4. Conclusions

In conclusion, for the first time, nanoporous membranes with high H/V selectivity without the insertion of any functional group were demonstrated by the effective utilization of

RSC Advances Accepted Manuscript

the amphoteric properties of a PBI polymer. The nanoporous PBI membranes were fabricated by a simple and cost-effective approach. The selected PBI-10% membrane showed an H/V selectivity of ~133 with a high diffusion rate of protons. This membrane showed excellent VRFB cyclability in terms of EEs and capacity retention. The prolonged OCV decay curve and low capacity decay rate of the PBI-10% membrane are due to the low crossover of vanadium ions caused by the positively charged PBI, which repels bulky vanadium ions; on the other hand, small and highly mobile protons escape easily through the polymer matrix. Thus, we believe that nanoporous PBI membranes could be a futuristic replacement for expensive Nafion membranes in practical applications of VRFBs.

5. Acknowledgements

‡ This work was supported by the National Research Foundation of Korea Grant funded by the Korean Government (MSIP) (NRF-2011-C1AAA001-0030538).

6. References

[1] Q.A. Acton, Issues in Energy Research and Application: 2013 Edition, ScholarlyEditions, 2013.
[2] M. Skyllas-Kazacos, M. Rychcik, R.G. Robins, A.G. Fane, M.A. Green, New All-Vanadium Redox Flow Cell, J. Electrochem. Soc. 133 (1986) 1057–1058. doi:10.1149/1.2108706.
[3] M. Skyllas-Kazacos, F. Grossmith, Efficient Vanadium Redox Flow Cell, J. Electrochem. Soc. 134 (1987) 2950–2953. doi:10.1149/1.2100321.
[4] S.-J. Seo, B.-C. Kim, K.-W. Sung, J. Shim, J.-D. Jeon, K.-H. Shin, et al., Electrochemical properties of pore-filled anion exchange membranes and their ionic transport phenomena for vanadium redox flow battery applications, J. Membr. Sci. 428 (2013) 17–23. doi:10.1016/j.memsci.2012.11.027.
[5] X. Li, H. Zhang, Z. Mai, H. Zhang, I. Vankelecom, Ion exchange membranes for vanadium redox flow battery (VRB) applications, Energy Environ. Sci. 4 (2011) 1147–1160. doi:10.1039/C0EE00770F.

RSC Advances Accepted Manuscript

[6] H. Prifti, A. Parasuraman, S. Winardi, T.M. Lim, M. Skyllas-Kazacos, Membranes for Redox Flow Battery Applications, Membranes. 2 (2012) 275–306. doi:10.3390/membranes2020275.
[7] B. Schwenzer, J. Zhang, S. Kim, L. Li, J. Liu, Z. Yang, Membrane Development for Vanadium Redox Flow Batteries, ChemSusChem. 4 (2011) 1388–1406. doi:10.1002/cssc.201100068.
[8] J. Xi, Z. Wu, X. Qiu, L. Chen, Nafion/SiO2 hybrid membrane for vanadium redox flow battery, J. Power Sources. 166 (2007) 531–536. doi:10.1016/j.jpowsour.2007.01.069.
[9] S. Winardi, S.C. Raghu, M.O. Oo, Q. Yan, N. Wai, T.M. Lim, et al., Sulfonated poly (ether ether ketone)-based proton exchange membranes for vanadium redox battery applications, J. Membr. Sci. 450 (2014) 313–322. doi:10.1016/j.memsci.2013.09.024.
[10] D. Chen, M.A. Hickner, E. Agar, E.C. Kumbur, Anion Exchange Membranes for Vanadium Redox Flow Batteries, ECS Trans. 53 (2013) 83–89. doi:10.1149/05307.0083ecst.
[11] J. Li, Y. Zhang, L. Wang, Preparation and characterization of sulfonated polyimide/TiO2 composite membrane for vanadium redox flow battery, J. Solid State Electrochem. 18 (2014) 729–737. doi:10.1007/s10008-013-2309-7.
[12] D. Chen, M.A. Hickner, E. Agar, E.C. Kumbur, Selective anion exchange membranes for high coulombic efficiency vanadium redox flow batteries, Electrochem. Commun. 26 (2013) 37–40. doi:10.1016/j.elecom.2012.10.007.
[13] C. Ding, H. Zhang, X. Li, T. Liu, F. Xing, Vanadium Flow Battery for Energy Storage: Prospects and Challenges, J. Phys. Chem. Lett. 4 (2013) 1281–1294. doi:10.1021/jz4001032.
[14] S.C. Chieng, M. Kazacos, M. Skyllas-Kazacos, Modification of Daramic, microporous separator, for redox flow battery applications, J. Membr. Sci. 75 (1992) 81–91. doi:10.1016/0376-7388(92)80008-8.
[15] B. Tian, C.W. Yan, F.H. Wang, Proton conducting composite membrane from Daramic/Nafion for vanadium redox flow battery, J. Membr. Sci. 234 (2004) 51–54. doi:10.1016/j.memsci.2004.01.012.
[16] H. Zhang, H. Zhang, X. Li, Z. Mai, J. Zhang, Nanofiltration (NF) membranes: the next generation separators for all vanadium redox flow batteries (VRBs)?, Energy Environ. Sci. 4 (2011) 1676–1679. doi:10.1039/C1EE01117K.
[17] H. Zhang, H. Zhang, X. Li, Z. Mai, W. Wei, Silica modified nanofiltration membranes with improved selectivity for redox flow battery application, Energy Environ. Sci. 5 (2012) 6299–6303. doi:10.1039/C1EE02571F.
[18] X. Wei, Z. Nie, Q. Luo, B. Li, B. Chen, K. Simmons, et al., Nanoporous Polytetrafluoroethylene/Silica Composite Separator as a High-Performance All-Vanadium Redox Flow Battery Membrane, Adv. Energy Mater. 3 (2013) 1215–1220. doi:10.1002/aenm.201201112.
[19] H. Zhang, H. Zhang, F. Zhang, X. Li, Y. Li, I. Vankelecom, Advanced charged membranes with highly symmetric spongy structures for vanadium flow battery application, Energy Environ. Sci. 6 (2013) 776–781. doi:10.1039/C3EE24174B.
[20] X.L. Zhou, T.S. Zhao, L. An, L. Wei, C. Zhang, The use of polybenzimidazole membranes in vanadium redox flow batteries leading to increased coulombic efficiency and cycling performance, Electrochimica Acta. 153 (2015) 492–498. doi:10.1016/j.electacta.2014.11.185.

RSC Advances Accepted Manuscript

[21] Y. Tanaka, Ion Exchange Membranes: Fundamentals and Applications, Elsevier, 2015.
[22] S. Slade, S.A. Campbell, T.R. Ralph, F.C. Walsh, Ionic Conductivity of an Extruded Nafion 1100 EW Series of Membranes, J. Electrochem. Soc. 149 (2002) A1556–A1564. doi:10.1149/1.1517281.
[23] E.-Y. Choi, S.-H. Moon, Characterization of acrylic acid-grafted PP membranes prepared by plasma-induced graft polymerization, J. Appl. Polym. Sci. 105 (2007) 2314–2320. doi:10.1002/app.26421.
[24] D.J. Jones, J. Rozière, Recent advances in the functionalisation of polybenzimidazole and polyetherketone for fuel cell applications, J. Membr. Sci. 185 (2001) 41–58. doi:10.1016/S0376-7388(00)00633-5.
[25] J.R. Klaehn, T.A. Luther, C.J. Orme, M.G. Jones, A.K. Wertsching, E.S. Peterson, Soluble N-Substituted Organosilane Polybenzimidazoles, Macromolecules. 40 (2007) 7487–7492. doi:10.1021/ma062186d.
[26] D.Y. Xing, S.Y. Chan, T.-S. Chung, Molecular interactions between polybenzimidazole and [EMIM]OAc, and derived ultrafiltration membranes for protein separation, Green Chem. 14 (2012) 1405–1412. doi:10.1039/C2GC35134J.
[27] N.A. Lange, Lange's Handbook of Chemistry, McGraw-Hill, 1999.
[28] D.R. Lide, CRC Handbook of Chemistry and Physics, 83rd Edition, Taylor & Francis, 2002.
[29] S. Kim, T.B. Tighe, B. Schwenzer, J. Yan, J. Zhang, J. Liu, et al., Chemical and mechanical degradation of sulfonated poly(sulfone) membranes in vanadium redox flow batteries, J. Appl. Electrochem. 41 (2011) 1201–1213. doi:10.1007/s10800-011-0313-0.
[30] Z. Mai, H. Zhang, H. Zhang, W. Xu, W. Wei, H. Na, et al., Anion-Conductive Membranes with Ultralow Vanadium Permeability and Excellent Performance in Vanadium Flow Batteries, ChemSusChem. 6 (2013) 328–335. doi:10.1002/cssc.201200561.

RSC Advances Accepted Manuscript

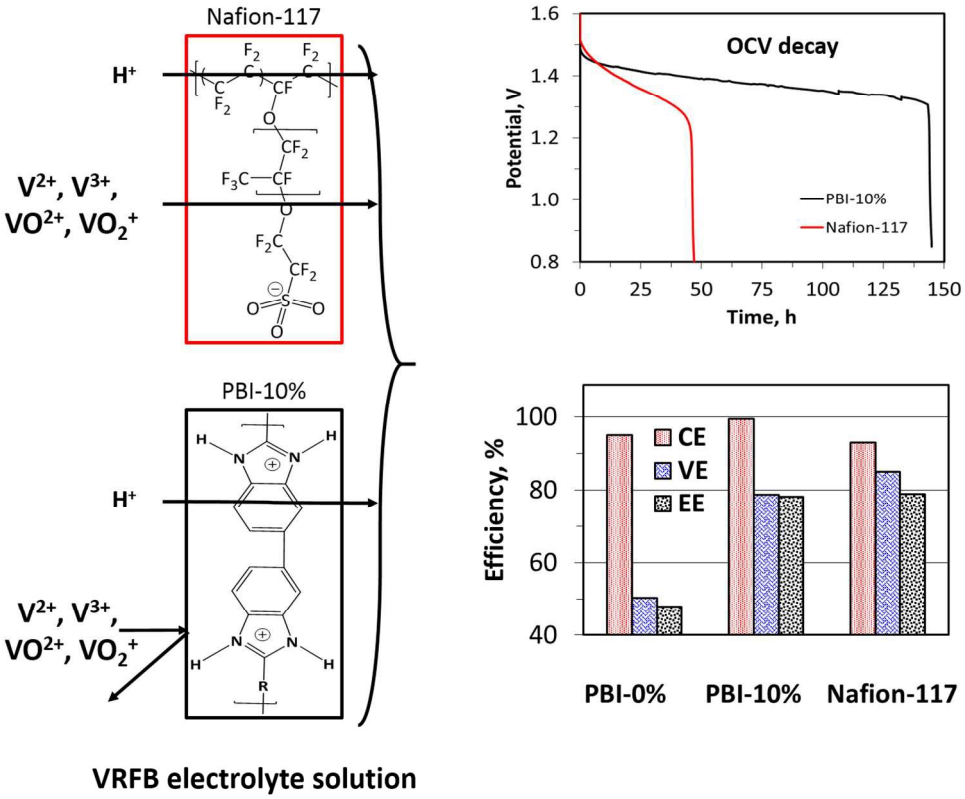

313x257mm (120 x 120 DPI)

RSC Advances Accepted Manuscript